The FEBS Journal

FEBS PRESS science publishing by scientists

Rewiring the yeast cell wall integrity (CWI) pathway through a synthetic positive feedback circuit unveils a novel role for the MAPKKK Ssk2 in CWI pathway activation

Elena Jiménez-Gutiérrez, Estíbaliz Alegría-Carrasco, Esmeralda Alonso-Rodríguez, Teresa Fernández-Acero, María Molina and Humberto Martín

Departamento de Microbiología y Parasitología, Facultad de Farmacia, Instituto Ramón y Cajal de Investigaciones Sanitarias (IRYCIS), Universidad Complutense de Madrid, Spain

Keywords
cell wall integrity; MAPK; phosphorylation; positive feedback loop; yeast

***Correspondence**
M. Molina and H. Martín, Departamento de Microbiología y Parasitología, Facultad de Farmacia, Universidad Complutense de Madrid, Plaza de Ramón y Cajal s/n, 28040-Madrid, Spain
Tel: +34 913941888
E-mails: molmifa@ucm.es (MM); humberto@ucm.es (HM)

(Received 22 November 2019, revised 17 February 2020, accepted 6 March 2020)

doi:10.1111/febs.15288

The cell wall integrity (CWI) pathway mediates the response of *Saccharomyces cerevisiae* to cell wall alterations. Stress at the cell surface is detected by mechanosensors, which transduce the signal to a protein kinase cascade that involves Pkc1, Bck1, Mkk1/Mkk2, the mitogen-activated protein kinase (MAPK) Slt2 and the transcription factor Rlm1. We incorporated a positive feedback loop into this pathway by placing a hyperactive *MKK1* allele under the control of the Rlm1-regulated *MLP1* promoter. This circuit operates as a signal amplifier and leads to a highly increased Slt2 activation under stimulating conditions. Triggering the CWI pathway in cells engineered with this circuit, which we have named the Integrity Pathway Activation Circuit (IPAC), results in strong growth inhibition. Exploitation of this hypersensitive phenotype allowed the identification of novel proteins that contribute in signalling to Rlm1 in response to cell surface stressing agents such as Congo red, zymolyase and SDS. Among these proteins, the MAPK kinase kinase Ssk2 of the osmoregulatory high-osmolarity glycerol (HOG) pathway, but not its paralogue Ssk22, proved to be necessary for the SDS-induced IPAC-mediated growth inhibition. We found the existence of an Ssk1-independent Ssk2-Pbs2-Hog1-CWI pathway signalling axis that contributes to Slt2 activation in response to cell surface stress. We also demonstrated that the MAP kinase kinases Mkk1 and Pbs2 and the MAPKs Slt2 and Hog1 of the HOG and CWI pathways interact physically, forming a complex. Our results show how a simple synthetic circuit can be used as a powerful tool for a better understanding of signalling pathways.

Introduction

Eukaryotic cells rely on mitogen-activated protein kinase (MAPK) pathways to mediate the response to a wide array of extracellular stimuli. Therefore, these routes regulate key cell fate decisions such as growth, differentiation or survival in response to stress [1]. They are very versatile signalling tools and contain a three-tiered protein kinase cascade comprising a MAP kinase kinase kinase (MAPKKK), a MAP kinase

Abbreviations
CWI, cell wall integrity; HOG, high-osmolarity glycerol; IPAC, Integrity Pathway Activation Circuit; MAPK, mitogen-activated protein kinase; OD, optical density; SD, synthetic dextrose; SDS, sodium dodecyl sulphate; SG, synthetic galactose; SR, synthetic raffinose; YPD, yeast extract–bacto-peptone–dextrose.

kinase (MAPKK) and a MAP kinase (MAPK), which are activated by sequential phosphorylation upon pathway stimulation. This multilayered structure provides a great flexibility of system response and allows signal amplification, multiple points of regulation, noise tolerance and the generation of switch-like responses [2].

The model yeast *Saccharomyces cerevisiae* has five MAPK pathways involved in mating, filamentous and invasive growth, spore wall assembly, osmoregulation and cell wall integrity (CWI) maintenance [2]. The CWI pathway is essential for cells to survive under cell wall stress conditions by triggering a salvage mechanism to strengthen this vital structure. This pathway is stimulated through a family of cell surface mechanosensors coupled to the Rho1 GTPase, which activates Pkc1, which in turn activates the CWI MAPK module, composed of the MAKKK Bck1, the MAPKKs Mkk1 and Mkk2, and the MAPK Slt2 [3]. Slt2 phosphorylates the MADS-box transcription factor Rlm1 [4], which induces the expression of cell wall maintenance proteins including the Slt2 paralogue Mlp1 [5]. The CWI pathway is also activated by heat stress, hypo-osmotic shock, oxidative stress, high and low pH, pheromones or DNA-damaging agents, indicating its involvement in the response to stresses and cellular processes not directly related to the cell wall [6].

The high-osmolarity glycerol (HOG) pathway maintains osmotic equilibrium under hyperosmotic stress [7]. This pathway is composed of two branches [8,9]. The first branch includes the transmembrane protein Sho1, the osmosensors Hkr1 and Msb2, and the membrane anchor protein Opy2, which transmit the signal to the MAPKKK Ste11 through the GTPase Cdc42, the adaptor protein Ste50 and the protein kinase Ste20 [9]. The second branch is initiated by the osmosensor histidine kinase Sln1, which signals through the phosphotransfer protein Ypd1 to the response regulator Ssk1, which activates the redundant MAPKKKs Ssk2 and Ssk22. The two branches converge in the phosphorylation of MAPKK Pbs2 by the corresponding MAPKKs. Therefore, the activation of any of these branches triggers the Pbs2-mediated phosphorylation of the MAPK Hog1 and its nuclear internalisation by the karyopherin-beta importin homologue Nmd5 [10]. Nuclear phosphorylated and thereby activated Hog1 phosphorylates several transcription factors to regulate the expression of genes involved in intracellular glycerol accumulation [11].

The CWI and HOG pathways do not operate in an isolated manner. The existence of crosstalk between them has been found in different conditions. The activation of Slt2 observed in response to hyperosmotic shock occurs in a HOG-dependent manner [12]. Moreover, Slt2 activation induced by the cell wall-damaging enzymatic complex zymolyase requires the participation of the Sho1 branch of the HOG pathway [13]. The interaction between Ste11 and Mkk1/2 through the protein Nst1 has been also reported [14]. In addition, some components of these pathways, apart from transmitting the signal to downstream elements, may play important roles in other processes, such as actin cytoskeleton organisation and cell polarity. For example, heat stress promotes the transient and reversible disassembly of the actin cytoskeleton. Pkc1, but not the downstream CWI MAPK cascade, is necessary for actin repolarisation [15]. After local cell wall damage, Pkc1 disperses polarity factors from the bud to wound sites through the induction of the formin Bni1 degradation [16]. Following osmotic stress, the MAPKKK Ssk2 mediates recovery of the actin cytoskeleton by forming a complex with actin, which requires the polarisome proteins Bud6 and Pea2, and the formin Bni1 [17].

Since the duration, timing and intensity of signalling through MAPK pathways are essential to produce the correct physiological output, loss of regulation of MAPK activity in mammalian cells is implicated in cancer and many other diseases [18]. In yeast, either the lack of CWI signalling in the presence of stress or the hyperactivation of the pathway leads to lethality [19]. Therefore, multiple fundamental mechanisms have evolved to achieve a precise modulation of these routes, including positive and negative feedback loops [20]. Whereas adaptation and noise resistance are typically brought by negative feedback mechanisms, positive feedback loops provide amplification, change the timing of the response and also trigger a bistable switch [21].

Their complexity and the importance in assuring cell survival under stress conditions make MAPK pathways very interesting targets for synthetic approaches. In addition, yeast is a very attractive model organism for these studies, since it has many valuable traits for synthetic biology [22]. For these reasons, a significant number of synthetic biology strategies have been applied to MAPK pathways in yeast, allowing a deeper understanding of signalling design principles [23]. In particular, synthetic feedback loops have been integrated within the mating pathway to provide several different behaviours, including bistability [24]. Here, we explore the consequences of introducing a synthetic positive feedback loop in the CWI pathway. Switching on this loop through the stimulation of the pathway leads to cellular lethality. We demonstrate the

potential of this genetic circuit as a tool for uncovering novel regulatory components of signalling through the CWI pathway.

Results

Rewiring the Slt2 MAPK module through a synthetic positive feedback circuit

To construct a positive feedback circuit that operates in the CWI pathway, the constitutively active *MKK1*^{S386P} allele [25] was placed between the *MLP1 (KDX1/YKL161C)* promoter, which is strongly induced following stimulation of this pathway [5], and the *ADH1* transcriptional terminator in a centromeric plasmid. In wild-type cells transformed with this plasmid, under stimulating conditions, the Rlm1-mediated induction of the *MLP1* promoter should give rise to a high amount of Mkk1^{S386P}, which would further phosphorylate and activate Slt2, providing activation of the feedback mechanism and resulting in continuous signal amplification (Fig. 1A).

We tested the impact of this circuit on signalling through the CWI pathway by analysing *MLP1* expression as readout. To this end, we determined β-galactosidase activity from a *MLP1-lacZ* reporter in cells carrying the genetic circuit in a centromeric plasmid versus those transformed with the empty vector, in response to concentrations ranging from 1 to 180 μg·mL^{-1} of the cell wall stressing agent Congo red for 4 h. In the absence of the circuit, successive increases in Congo red concentration resulted in increases in β-galactosidase levels of fourfold (1 μg·mL^{-1}), 25-fold (5 μg·mL^{-1}), 110-fold (30 μg·mL^{-1}) and 95-fold (180 μg·mL^{-1}; Fig. 1B), indicating a saturated response from a concentration of 30 μg·mL^{-1}. The presence of the feedback circuit clearly increased the β-galactosidase values in relation to cells bearing the empty vector, with the highest amplification at 5 μg·mL^{-1} of Congo red (~ 4-fold). We also determined the impact of this genetic circuit on the dual phosphorylation, and therefore activation, kinetics of the MAPK Slt2 in response to the treatment with low, medium and high Congo red concentration for up to 8 h. As observed in Fig. 1C, at the lowest Congo red concentration the amount of activated Slt2 peaked at 8 h; at higher concentrations, Slt2 phosphorylation reached the maximum level at shorter times, between 2 and 4 h. In cells without the circuit, maximum activation ranged from twofold following treatment with 1 μg·mL^{-1} to eightfold with 180 μg·mL^{-1}. In all cases, the circuit significantly increased the amount of phosphorylated Slt2 (Fig. 1C). At 180 μg·mL^{-1}, an increase of 16-fold over the basal phosphorylation in cells lacking the circuit at time 0 was observed. These results indicate that the genetic loop is indeed functional in promoting a high and sustained signalling flow through the CWI pathway. Thus, we named this circuit 'IPAC' standing for 'Integrity Pathway Activation Circuit'.

We next explored the effect of this circuit on signalling through the pathway in response to hypotonic shock, which induces a very rapid and transient activation of the CWI pathway [26]. As observed in Fig. 1D, IPAC-containing cells displayed similar Slt2 phosphorylation kinetics to cells lacking the circuit, peaking at 1 min, but with higher phospho-Slt2 levels at any time point. This result shows the rapidity of the IPAC in developing an amplified response and the maintenance of adaptation mechanisms to hypotonic shock in the IPAC-rewired CWI pathway. We then analysed the effect of eliminating the Mid2 sensor, which mediates most of the Congo red-induced CWI pathway activation [27]. Deletion of *MID2* significantly reduced *MLP1-lacZ* transcriptional activation in IPAC-containing cells after treatment with Congo red (Fig. 1E). However, whereas the presence of the IPAC doubled β-galactosidase levels upon Congo red treatment, the increase was sevenfold in *mid2*Δ mutants. These results suggest first that the IPAC-rewired CWI pathway keeps its sensitivity to regulators of the pathway and second that the capacity of the IPAC for increasing signalling is higher under conditions promoting low activation.

The positive feedback loop renders cells hypersensitive to CWI pathway activation

We next wondered whether the activation of the IPAC affected cell growth. As expected, the presence of agents that disturb the yeast cell surface, namely Congo red, SDS or zymolyase, prevented *slt2*Δ mutant cells from growing (Fig. 2A). These compounds also led to growth inhibition of IPAC-containing cells, although to a lesser extent as compared to the *SLT2* deletion. This inhibition was observed at concentrations that did not affect growth of wild-type cells. This result indicates that the IPAC enhances the sensitivity of yeast to cell wall stress and is consistent with the reported growth inhibition caused by *GAL1*-driven overexpression of the hyperactive allele *MKK1*^{S386P} that is part of the circuit [25]. Caffeine was shown to activate the MAPK Slt2 but not the transcription factor Rlm1 [28]. As observed in Fig. 2A, this compound led to growth inhibition of *slt2*Δ but not IPAC-containing cells, confirming that there is no significant Rlm1-dependent *MLP1* gene

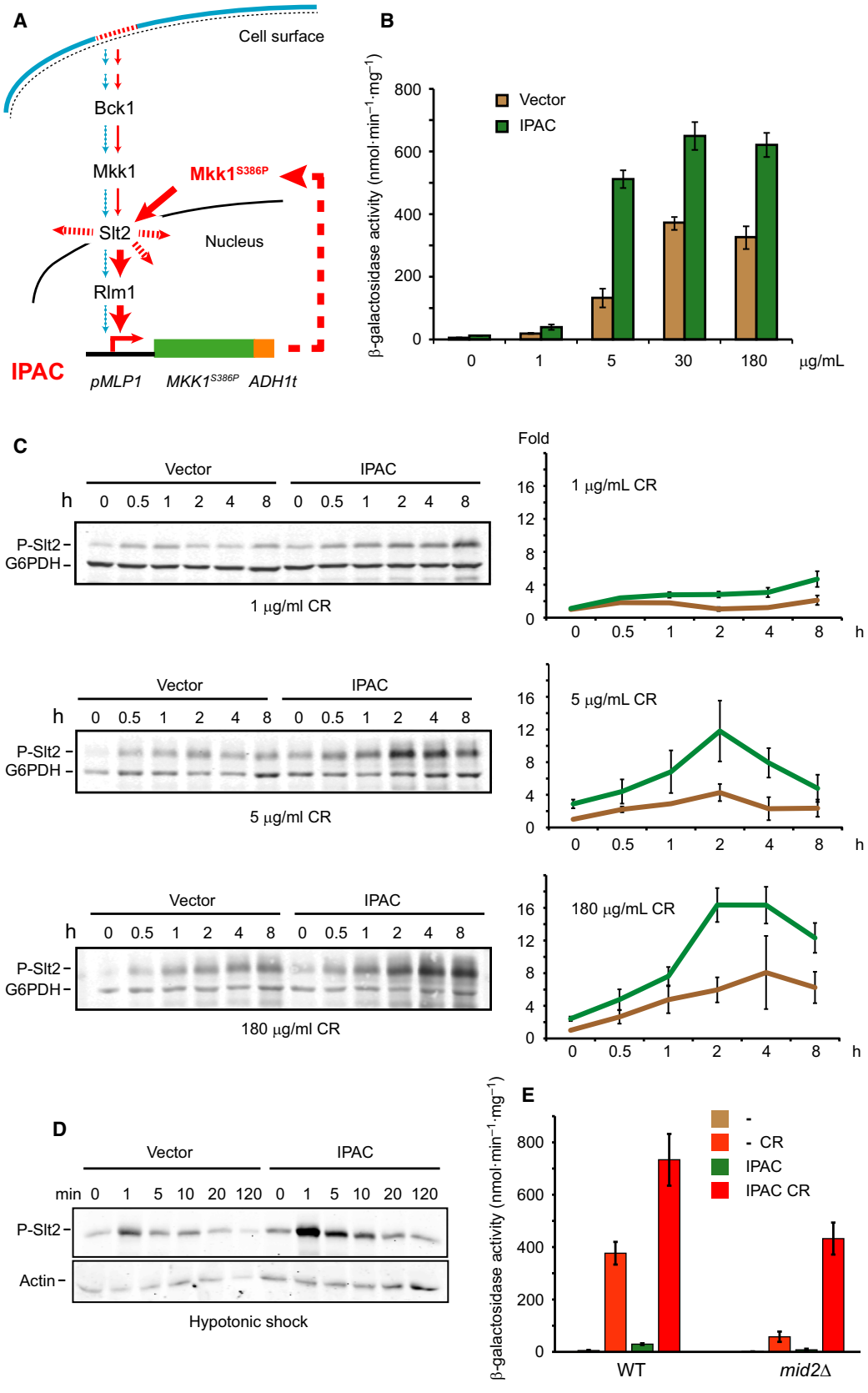

Fig. 1. The IPAC promotes hyperactivation of the CWI pathway following cell wall stress. (A) Scheme of the CWI pathway containing the IPAC. IPAC consists of the *MLP1* promoter, the hyperactive allele $MKK1^{S386P}$ and the transcription termination sequence of *ADH1* (*ADH1t*). In the absence of stimulus, the pathway displays a low basal level of signalling (blue lines). Stimulation of the pathway (red lines) leads to Slt2 activation by dual phosphorylation, resulting in *MLP1* transcriptional induction via Rlm1 activation. *MLP1*-driven $MKK1^{S386P}$ expression provokes an increase in Slt2 activation, generating a positive feedback loop and the hyperactivation of the CWI pathway. (B) Expression of *MLP1-lacZ*, determined as β-galactosidase activity from extracts of the strain BY4741 cotransformed with the plasmid p*MLP1-lacZ* and either the empty vector YCplac111 or YCplac111-IPAC. Cells were grown in YPD medium at 24 °C in the absence (–) or presence of the indicated concentrations of Congo red (CR) for 4 h. Data represent the average of β-galactosidase activity of three independent transformants. Error bars indicate standard deviation. (C) Western blotting analysis of extracts of the same BY4741 cells as in (B), cultured in YPD at 24 °C and treated with the indicated concentrations of CR for the indicated times (h). Dually phosphorylated Slt2 and G6PDH (as a loading control) were detected with anti-phospho-p44/42 and anti-G6PDH antibodies, respectively. A representative blot is included. The graphics show the amount of phosphorylated Slt2, normalised with respect to the loading control for each sample and expressed as fold increase relative to the wild-type level (Vector) in the absence of stress. Data represent the average of three independent transformants. Error bars indicate standard deviation. (D) Western blotting analysis of extracts of BY4741 cells transformed with either the empty vector YCplac111 or YCplac111-IPAC. Aliquots of a single culture in YPD plus 1 M sorbitol were withdrawn before (0) and after the indicated times following resuspension in YPD. Dually phosphorylated Slt2 and actin (as a loading control) were detected with anti-phospho-p44/42 and anti-actin antibodies, respectively. A representative blot from three different experiments is shown. (E) CR signalling in IPAC-containing cells is sensed and modulated similarly to wild-type cells. β-Galactosidase activity of cell extracts from BY4741 (WT) and the isogenic *mid2*Δ strains bearing the p*MLP1-lacZ* plasmid and YCplac111 (–) or YCplac111-IPAC. Cells were either left untreated (–) or treated for 4 h with 30 $\mu g \cdot mL^{-1}$ of CR. Data represent the average of β-galactosidase activity of three independent transformants. Error bars indicate standard deviation.

induction. The IPAC also strongly affected growth in liquid media containing cell wall-altering agents, as reflected by the reduction in the MIC (minimal inhibitory concentration) of zymolyase observed in IPAC-bearing cells when compared to cells lacking the circuit (Fig. 2B). Since Congo red-induced *MLP1* transcriptional induction is abolished in *rlm1*Δ cells [5], we wondered whether IPAC-containing *rlm1*Δ cells no longer showed Congo red sensitivity. This was the case, as observed by using a halo assay (Fig. 2C), proving that the IPAC-mediated sensitivity of yeast cells to CWI stimuli such as Congo red is dependent on the full functionality of this signalling circuit. These results also indicate that the IPAC is an excellent tool for analysing CWI pathway signalling through an easy growth assay.

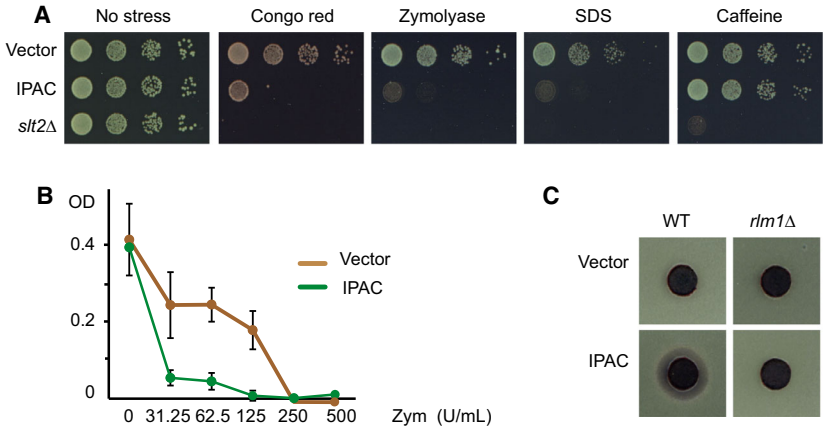

Fig. 2. Activation of the IPAC leads to growth inhibition. (A) Ten-fold serial dilutions of the BY4741 strain transformed with the empty vector YCplac111 or YCplac111-IPAC and the isogenic *slt2*Δ strain carrying YCplac111. Yeast cells were spotted onto SD Leu– plates pH 6.5 in the absence (no stress) or presence of 3 $\mu g \cdot mL^{-1}$ of CR, 10 $U \cdot mL^{-1}$ of zymolyase, 100 $\mu g \cdot mL^{-1}$ SDS or 4 mM of caffeine and incubated at 30 °C for 48 h. A representative assay from three different experiments with distinct transformants is shown. (B) Multiwell plate sensitivity assay of the BY4741 strain transformed with YCplac111 or YCplac111-IPAC to the indicated concentrations of zymolyase. Data represent the average value of three independent transformants. Error bars indicate standard deviation. (C) Growth inhibition halo assay on SD Leu– plates of strains BY4741 or the isogenic Y00993 (*rlm1*Δ) strains transformed with YCplac111 or YCplac111-IPAC. Six-millimetre-diameter discs were impregnated with 20 μL of 10 $mg \cdot mL^{-1}$ CR. A representative assay from three different experiments with distinct transformants is shown.

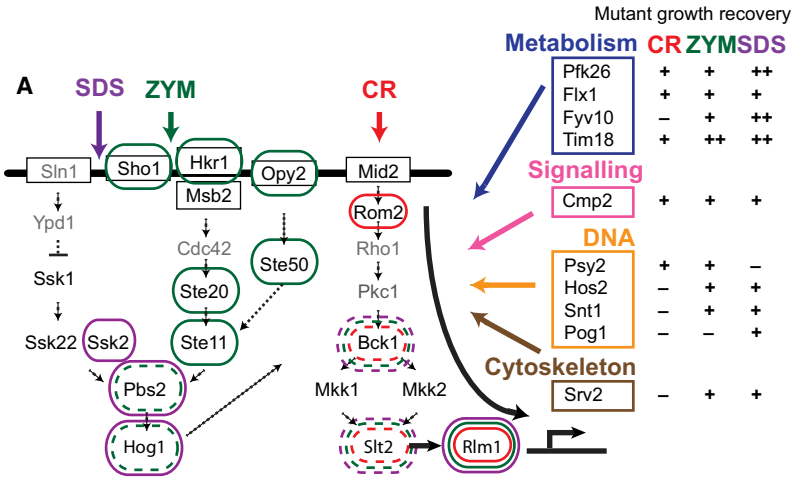

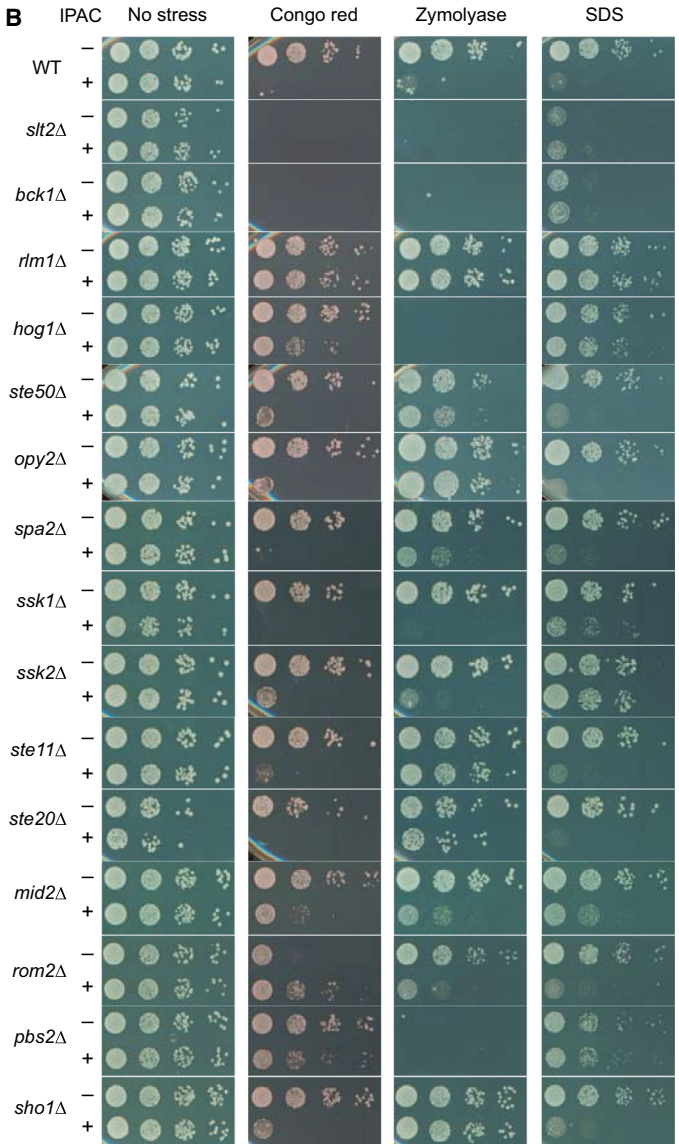

Fig. 3. Results of the screening of a subcollection of *Saccharomyces cerevisiae* mutants able to suppress the lethality of IPAC-engineered cells treated with CR, zymolyase and SDS. (A) Proteins of the HOG and CWI pathway surrounded by red, green and purple circles indicate that the corresponding mutants recovered growth under CR, zymolyase and SDS stress, respectively. Discontinuous circles indicate that the corresponding mutant without the IPAC was already sensitive to the stress. Mutants lacking proteins in grey were not analysed. Novel genes identified in the screening whose mutation was able to recover growth are indicated on the right. The scores for growth recovery under each stress are indicated, ranging from strong recovery (++) to no effect (–) according to spot assays shown in Fig. 4A. (B) Sensitivity of wild-type BY4741 and the indicated isogenic mutant strains bearing the vector pHR70 (–) or the plasmid pHR70-IPAC (+) to different stresses. Ten-fold serial dilutions of cell suspensions were spotted onto SD Ura– pH 6.5 plates in the absence (no stress) or presence of 5 $\mu g \cdot mL^{-1}$ of CR, 10 $U \cdot mL^{-1}$ (50 $\mu g \cdot mL^{-1}$) of zymolyase or 100 $\mu g \cdot mL^{-1}$ of SDS, and incubated at 30 °C for 48 h. A representative assay from three different experiments with distinct transformants is shown.

IPAC-based identification of novel proteins that contribute to signalling through the CWI pathway

In view of the previous results, we considered IPAC an excellent tool to identify regulators of the CWI pathway. We reasoned that any mutation that promotes a significant reduction in signalling would restore growth of IPAC-containing cells under CWI stimulation. To evaluate this, a subcollection of 265 mutant strains deleted in genes related to signalling or apoptosis (Table S1) and transformed with the centromeric plasmid YCplac111-IPAC was screened for their ability to grow in the presence of low concentrations of Congo red, zymolyase or SDS (see Materials and methods). Forty of these mutants were selected on this basis, and 25 of them reproduced some growth recovery phenotype after *de novo* transformation with a different centromeric plasmid containing the IPAC. Ten mutants were affected in genes encoding potential novel CWI pathway regulators under cell wall stress (Figs 3A and 4A). The effect of these 10 mutations on CWI pathway signalling was analysed by using the *MLP1-lacZ*-based transcriptional reporter assay (Fig. 4B). The *rlm1*Δ and *hkr1*Δ mutants were also included as controls. Lack of Rlm1 resulted in the absence of *MLP1* induction in response to Congo red, zymolyase and SDS, whereas the absence of the HOG pathway osmosensor Hkr1 only blocked zymolyase induction, as expected according to its role in sensing this cell wall stressor [13]. It is interesting to note that four out of these 10 mutants lack metabolic enzymes, and another four are defective in proteins related to DNA function.

Among the 25 identified mutants, 15 were affected in signalling components already known to participate in MAPK signalling (Fig. 3A,B). A detailed analysis of the effect of these mutations on IPAC-induced growth inhibition provided interesting information about the signalling flow to Slt2 promoted by these stresses. The most interesting data came from observing growth of yeast mutants in the presence of SDS. The lack of the Rho1 GEF Rom2 did not recover growth of cells carrying the circuit under SDS stress, supporting the idea that, as with zymolyase, signalling to Slt2 in response to this stress does not go through the conventional path followed by other cell wall stresses. Deletion of *PBS2* and *HOG1* recovered growth of cells carrying the IPAC on SDS-containing media, also suggesting the involvement of the HOG pathway in signal transmission from the cell surface to the CWI pathway in response to this membrane insult (Fig. 3A, B). Most interestingly, and in contrast to that occurring with zymolyase, deletion of *SSK2* but not *SHO1, STE20* or *STE50* promoted the growth of IPAC-bearing cells under SDS stress, suggesting the existence of a novel pathway for signalling to Slt2 that is mediated by the MAPKKK Ssk2.

Ssk2 is necessary for full Slt2 activation in response to SDS

In order to analyse the role of Ssk2 in signalling through the CWI pathway in response to SDS, we first studied the time course of Slt2 phosphorylation and *MLP1* induction in cells stressed with the detergent. As observed in Fig. 5A, SDS promoted a very fast activation of Slt2. This high and rapid Slt2 phosphorylation peaked at 1 min, declined after this time and then slowly increased to reach a maximum at 120 min. Whereas the first burst of Slt2 phosphorylation was not affected in *ssk2*Δ mutants, the long-term activation significantly diminished in comparison with wild-type cells. This reduction in the amount of phosphorylated Slt2 was also observed in cells lacking either Pbs2 or Hog1 (Fig. 5A). Moreover, SDS-induced *MLP1-lacZ* expression was severely reduced in both *ssk2*Δ and *hog1*Δ mutants (Fig. 5B). Interestingly, Hog1 also seemed to contribute in signalling to Slt2 in response to Congo red, since signalling was reduced by the half in mutants lacking this MAPK. In summary, these results indicate that SDS triggers firstly a very fast and transient activation of the CWI pathway and, secondly, a slow and sustained response that is significantly mediated by Ssk2, Pbs2 and Hog1.

Phosphorylation of Slt2 under 1 M sorbitol treatment has also been described to be Pbs2-dependent [12]. In order to explore whether Ssk2 is involved in this activation, we performed an analysis of Slt2 phosphorylation in response to this osmotic stress in WT and *ssk2*Δ strains. As shown in Fig 5C, the absence of Ssk2 did not altered either the amount of phosphorylated Slt2 or the activation time course, indicating that this stress is not routed through this MAPKKK to Slt2.

Heat stress activation of the CWI pathway involves superficial redistribution of some components operating in the CWI pathway, such as Rho1, likely to repair cell wall damage [15]. In the absence of stress, Pkc1 is localised at sites of polarised growth, namely bud necks at cytokinesis and emerging bud tips [29,30]. Following a cell wall stress, Pkc1 relocalises to specific regions beneath the cell surface [29]. Then, Rho1-GTP activates Pkc1, which in turn activates the downstream MAP kinase cascade. We then studied the effect of SDS on Pkc1 subcellular localisation. As observed in Fig. 5D, SDS promoted relocalisation of Pkc1 to the

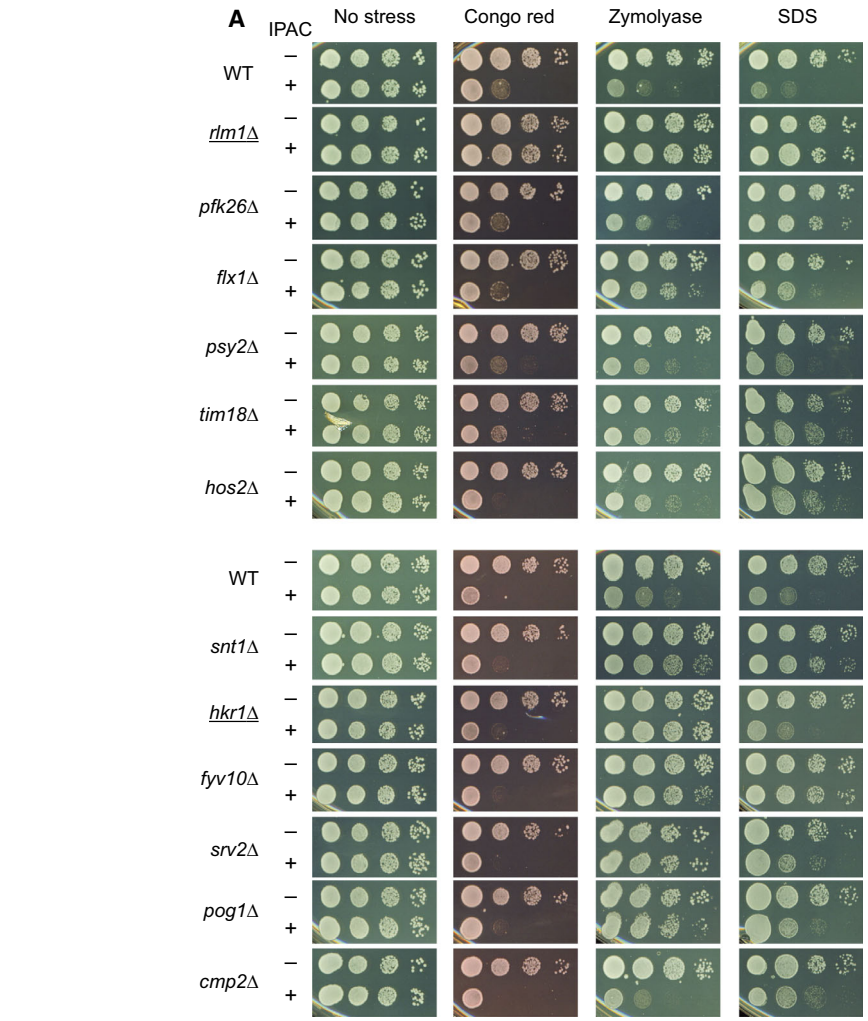

Fig. 4. Deletion of different genes reduces the sensitivity and transcriptional response of IPAC-containing cells to CWI pathway-activating compounds. (A) Sensitivity of BY4741 (WT) and the indicated isogenic mutant strains bearing the empty vector pHR70 (–) or plasmid pHR70-IPAC (+) to different stresses. Ten-fold serial dilutions of cell suspensions were spotted onto SD Ura– pH 6.5 plates in the absence (no stress) or presence of 10 $\mu g \cdot mL^{-1}$ of CR, 150 $\mu g \cdot mL^{-1}$ of zymolyase or 100 $\mu g \cdot mL^{-1}$ of SDS, and incubated at 30 °C for 48 h. A representative assay from three different experiments is shown. Mutant strains used as controls are underlined. (B) Transcriptional response of BY4741 (WT) and the indicated isogenic mutant strains transformed with the p*MLP1-lacZ* plasmid. β-Galactosidase activity was determined in the absence (–) or presence of CR (30 $\mu g \cdot mL^{-1}$ for 4 h), zymolyase (8 $\mu g \cdot mL^{-1}$ for 4 h) or SDS (100 $\mu g \cdot mL^{-1}$ for 4 h). Data represent the average of the activity of three independent transformants as the percentage relative to the WT strain (100%). Mutant strains used as controls are underlined. Error bars indicate the standard deviation. One asterisk indicates a *P*-value of < 0.05 using Student's *t*-test.

bud periphery. However, this effect was independent of the presence of Ssk2 (see Fig. 5D). Therefore, Ssk2 does not seem to affect the formation of plasma membrane-associated CWI pathway signalling complexes upon SDS stress.

Ssk2 activation leads to CWI stimulation via Pbs2/Hog1

To learn more about this novel pathway towards Slt2, we next analysed the ability of a constitutively activated Ssk2-mediated branch of the HOG pathway to trigger Slt2 activation. Overexpression of $Ssk2^{\Delta N}$, a constitutively active Ssk2 version lacking the N-terminal regulatory domain [31,32], resulted in a Bck1-dependent phosphorylation of Slt2 that also required Pbs2 and Hog1 (Fig. 6A). In contrast, removal of any of the GEF proteins for Rho1, namely Rom1, Rom2 or Tus1, did not block $Ssk2^{\Delta N}$-induced Slt2 activation. Moreover, growth inhibition promoted by overexpression of this Ssk2 version was abolished in *pbs2*Δ and *hog1*Δ mutants, even in the presence of the IPAC (Fig. 6B). These results indicate that the activation of Ssk2 results in Slt2 phosphorylation via the Pbs2-Hog1 kinase module. $Ssk2^{\Delta N}$-triggered Slt2 activation required both the phosphorylation and the catalytic activity of Hog1, as evidenced by the lack of Slt2 activation observed in cells expressing the kinase-dead ($Hog1^{K52M}$) and the nonphosphorylatable ($Hog1^{T174A,Y176A}$) mutant versions (Fig. 6C). In order to further explore the connection between the HOG and CWI pathways, we also constructed the constitutively active version of Pbs2, $Pbs2^{EE}$. This version contains glutamic residues instead of the serine 514 and threonine 518, whose changes to aspartic residues were previously described to activate Pbs2 without the involvement of upstream elements by mimicking phosphorylation events [31]. Galactose-induced expression of $Pbs2^{EE}$ did not lead to growth inhibition in wild-type, but promoted lethality in IPAC-engineered cells, indicating that Pbs2-promoted signalling was transmitted to the CWI MAPK module. As expected, under these conditions *SSK2* deletion did not affect IPAC activation, but removal of either Hog1 or Bck1 strongly reduced IPAC-induced growth inhibition (Fig. 6D), confirming that the signal flows through Hog1 and Bck1.

The lack of any of the transcription factors operating downstream of Hog1, including Hot1, Smp1, Msn2, Msn4, Msn1, the transcription repressor Sko1 and the Hog1-substrate kinase Rck2 [7], did not alleviate the SDS-induced growth inhibition of IPAC-bearing cells (not shown). In fact, the Hog1-dependent signalling to Slt2 does not rely on any of its nuclear functions, since deletion of the gene coding for the Hog1 importin Nmd5 [10] neither affected SDS or Congo red activation of CWI signalling, as determined by *MLP1p-lacZ* transcriptional reporter induction (Fig. 7A), nor growth inhibition in IPAC-bearing cells (Fig. 7B) or Slt2 phosphorylation (Fig. 7C). In line with this, SDS treatment did not lead to Hog1 translocation to the nucleus, in contrast to that observed under osmotic shock (Fig. 7D).

The MKKs and MAPKs of the HOG and CWI pathways form a protein complex

The fact that it is not necessary for Hog1 to be translocated to the nucleus for signalling to Slt2 suggests that the Pbs2-Hog1 module could be directly regulating components of the CWI pathway. We then analysed the existence of physical interactions of Pbs2 and Hog1 with Mkk1 and Slt2. We used the GST-$Pbs2^{EE}$ expressing plasmid to explore whether Mkk1 and Slt2 interact with this MAPKK. As shown in Fig. 8A,B, GST-$Pbs2^{EE}$ was able to pull down both Slt2-myc and Mkk1-myc. GST-$Pbs2^{EE}$ also pulled down endogenous Slt2, as did GST-Slt2 and GST-Mkk1. Moreover, endogenous Hog1 copurified with GST-Slt2 and GST-Mkk1, as well as with GST-$Pbs2^{EE}$ (Fig. 8C). These results suggest physical interaction between these four proteins in a complex. Interestingly, interaction between GST-Mkk1 and GST-Slt2 with Hog1 was not impaired by the absence of Ssk2, Bck1, Mkk1/2, Slt2 or Pbs2 (Fig. 9), suggesting a direct binding of Hog1 to either Mkk1 or Slt2.

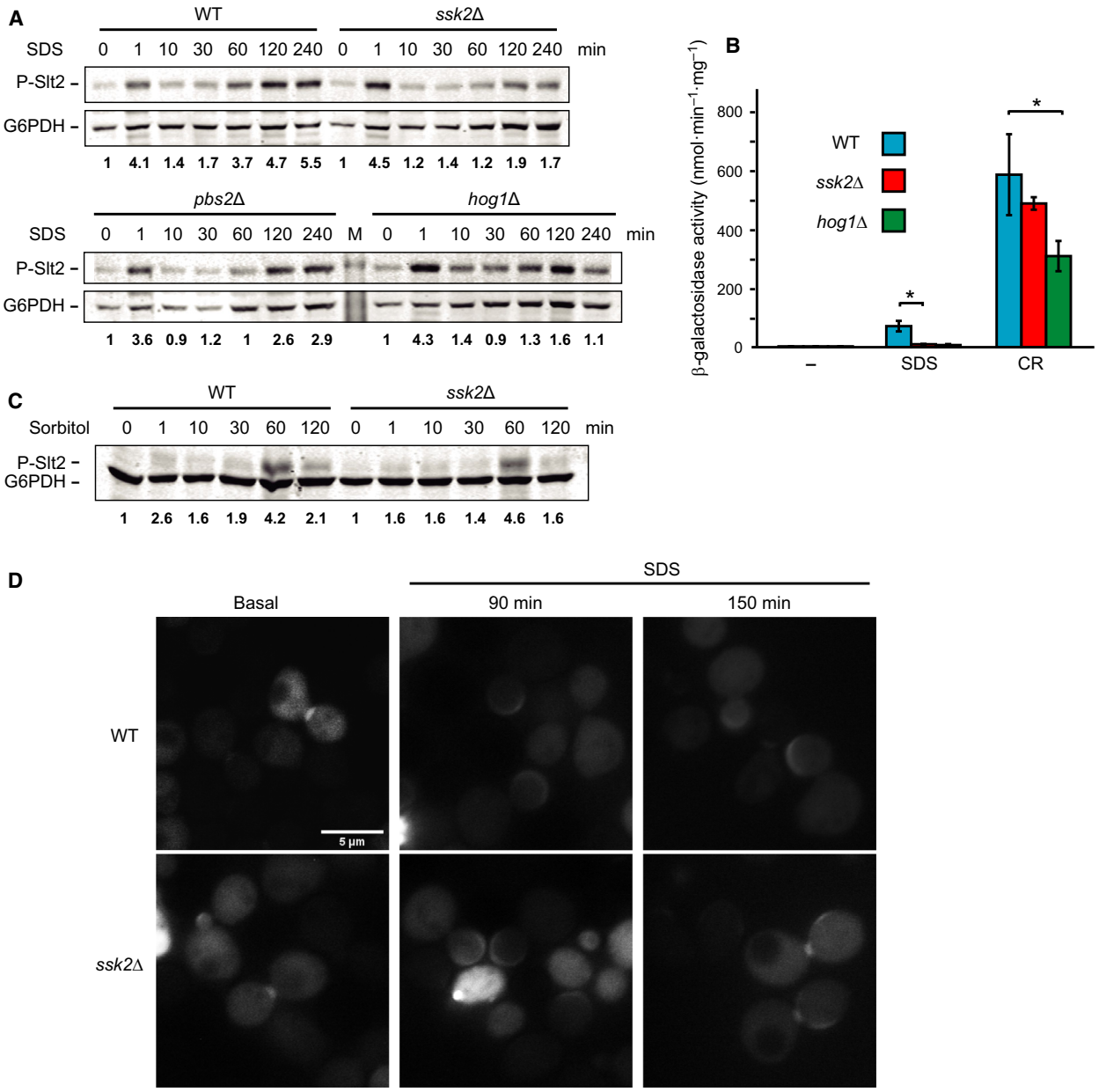

Fig. 5. *ssk2*Δ mutants show reduced signalling through the CWI pathway in response to SDS. (A) Western blotting analysis of extracts of BY4741 (WT), *ssk2*Δ, *pbs2*Δ and *hog1*Δ cells cultured in YPD at 30 °C and treated with 100 μg·mL^{-1} of SDS for the indicated times (min). Dually phosphorylated Slt2 and G6PDH (as a loading control) were detected with anti-phospho-p44/42 and anti-G6PDH antibodies, respectively. The numbers below show the amount of phosphorylated Slt2, normalised with respect to the loading control for each sample and expressed as fold increase relative to the level in the absence of stress. M corresponds to the lane loaded with the molecular weight protein marker. Representative blots from two independent experiments are shown. (B) β-Galactosidase activity of cell extracts from the wild-type strain BY4741 (WT) and the isogenic *ssk2*Δ and *hog1*Δ strains bearing the p*MLP1-lacZ* plasmid. Cells were either left untreated (–) or treated for 4 h with 100 μg·mL^{-1} of SDS or 30 μg·mL^{-1} of CR. Data represent the average of β-galactosidase activity of three independent transformants. Error bars indicate standard deviation and one asterisk a *P*-value of < 0.05 by two-tailed Student's *t*-test. (C) Western blotting analysis of extracts of BY4741 (WT) and *ssk2*Δ cells cultured in YPD at 30 °C and treated with 1 M sorbitol for the indicated times (min). Dually phosphorylated Slt2 and G6PDH (as a loading control) were detected as above. The numbers below show the amount of phosphorylated Slt2, normalised as in A. A representative blot from two independent experiments is shown. (D) Pkc1 localisation upon SDS treatment. Fluorescence microscopy images of BY4741 (WT) and the isogenic *ssk2*Δ mutant cells, both expressing Pkc1-GFP from plasmid pVD67, cultured in YPD in basal conditions or treated with 100 μg·mL^{-1} of SDS for the indicated times. Representative photographs from three different experiments are shown. Scale bar = 5 μM.

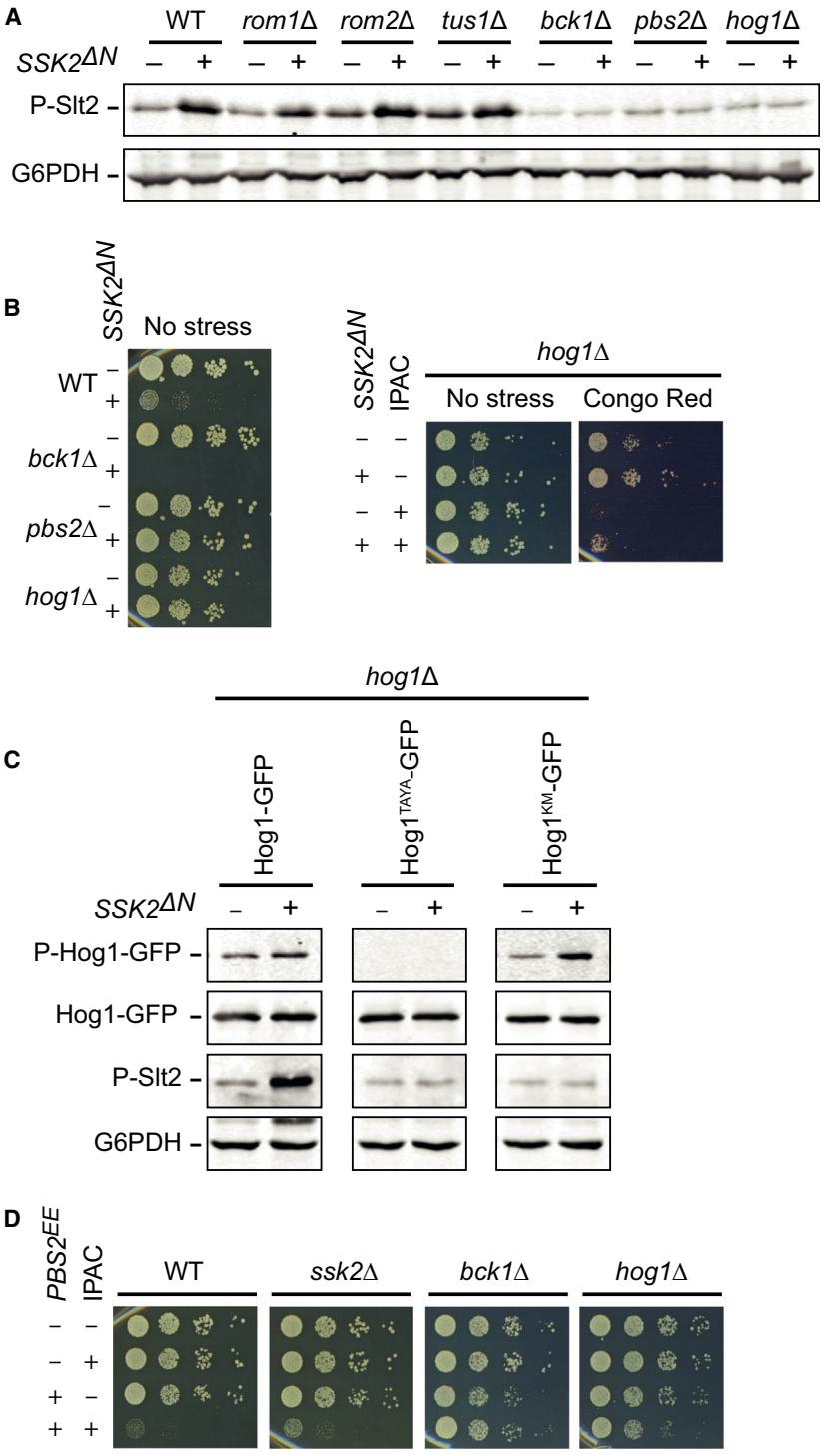

Fig. 6. Constitutive activation of the Ssk2 branch of the HOG pathway leads to CWI pathway activation. (A) Western blotting analysis of extracts of BY4741 (WT) and the isogenic *rom1*Δ, *rom2*Δ, *tus1*Δ, *bck1*Δ, *pbs2*Δ and *hog1*Δ strains expressing the constitutively active Ssk2$^{\Delta N}$ version (+) (pRS413-p*GAL1-SSK2*$^{\Delta N}$) or not (–) (pCW194). Cells were cultured in SG His– at 30 °C for 4 h. Dually phosphorylated Slt2 and G6PDH (as a loading control) were detected with anti-phospho-p44/42 and anti-G6PDH antibodies, respectively. (B) Ten-fold serial dilutions of BY4741 (WT), *bck1*Δ, *pbs2*Δ and *hog1*Δ expressing Ssk2$^{\Delta N}$ (+) (pRS413-p*GAL1-SSK2*$^{\Delta N}$) or not (–) (pCW194) spotted onto SG His– pH 6.5 plates without stress and incubated at 30 °C for 72 h (left panel). Ten-fold serial dilutions of *hog1*Δ cells expressing Ssk2$^{\Delta N}$ (+) (pRS413-p*GAL1-SSK2*$^{\Delta N}$) or not (–) (pCW194) and the IPAC (+) (YCplac111-IPAC) or not (–) (YCplac111), spotted onto SG His– Leu– pH 6.5 plates in the absence (no stress) or presence of 5 μg·mL^{-1} of CR, and incubated at 30 °C for 72 h (right panel). (C) Western blotting analysis of extracts of *hog1*Δ cells bearing *HOG1-GFP* (pRS416-*HOG1-GFP*), a nonphosphorylatable version (pRS416-*HOG1*^{TAYA}*-GFP*) and a kinase-dead version (pRS416-*HOG1*^{KM}*-GFP*) in combination with *SSK2*$^{\Delta N}$ (+) (pRS413-p*GAL1-SSK2*$^{\Delta N}$) or vector pCW194 (–). Cells were cultured in SG Ura– His– at 30 °C for 4 h. Phosphorylated Hog1, GFP-fused Hog1, dually phosphorylated Slt2 and G6PDH (as a loading control) were detected with anti-phospho-p38, anti-GFP, anti-phospho-p44/42 and anti-G6PDH antibodies, respectively. (D) Ten-fold serial dilutions of BY4741 (WT), *ssk2*Δ, *bck1*Δ and *hog1*Δ cells bearing pEG(KG)-*PBS2*^{EE} or pEG(KG) (–) and YCplac111-IPAC (+) or YCplac111 (–). Cell suspensions were spotted onto SG Ura– Leu– pH 6.5 plates and incubated at 30 °C for 72 h.

Discussion

Here, we demonstrated that engineering yeast cells with synthetic positive feedback loops constitutes an excellent approach for gaining insight into different aspects of MAPK signalling, such as identifying novel components involved in the response to a specific stress. Since hyperactivation of the CWI pathway leads to lethality [25], we reasoned that introduction of a structural gene coding a hyperactive kinase operating in this pathway under the control of a pathway-

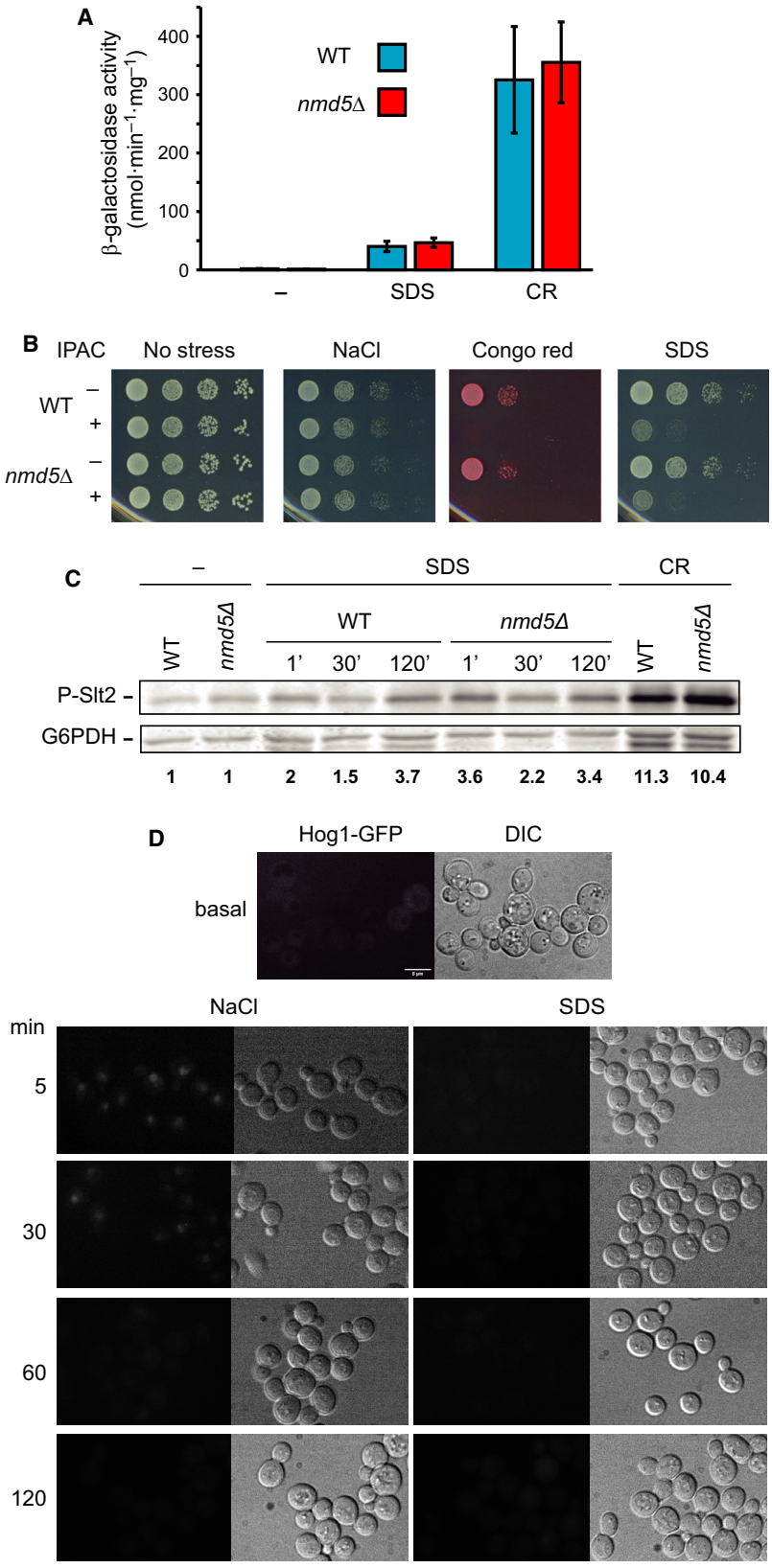

Fig. 7. Hog1 is not imported to the nucleus in response to SDS. (A) β-Galactosidase activity of cell extracts from the BY4742 (WT) and the isogenic APY276 (*nmd5*Δ) mutant strain, both bearing the p*MLP1-lacZ* vector. Cells were either left untreated (–) or treated for 4 h with 100 $\mu g \cdot mL^{-1}$ of SDS or 30 $\mu g \cdot mL^{-1}$ of CR. Data represent the average of β-galactosidase activity of three independent transformants. Error bars indicate standard deviation. (B) Ten-fold serial dilutions of BY4742 (WT) and the isogenic APY276 (*nmd5*Δ) mutant cells bearing the IPAC (+) (pHR70-IPAC) or not (–) (pHR70). Cell suspensions were spotted onto SD Ura– pH 6.5 plates in the absence (no stress) or presence of 0.8 M NaCl, 10 $\mu g \cdot mL^{-1}$ of CR and 100 $\mu g \cdot mL^{-1}$ of SDS, and incubated at 30 °C for 48 h. A representative assay is shown from two different experiments with distinct transformants. (C) Western blotting analysis of extracts of PW245 (WT) and the isogenic PW349 (*nmd5Δ*) mutant cells cultured in YPD at 30 °C for 2 h and treated with 100 $\mu g \cdot ml^{-1}$ of SDS for the indicated times (h) or 30 $\mu g \cdot mL^{-1}$ of CR for 4 h. Dually phosphorylated Slt2 and G6PDH (as a loading control) were detected with anti-phospho-p44/42 and anti-G6PDH antibodies, respectively. The numbers below show the amount of phosphorylated Slt2 normalised with respect to the loading control for each sample and expressed as fold increase relative to either the WT or *nmd5*Δ level in the absence of stress. A representative blot from two independent experiments is shown. (D) Fluorescence and DIC (differential interference contrast) microscopy of PW245 cells expressing Hog1-GFP, cultivated in YPD (basal) and treated with 0.9 M NaCl or 100 $\mu g \cdot mL^{-1}$ of SDS for the indicated times. Representative photographs from three independent experiments are shown. Scale bar = 5 μM.

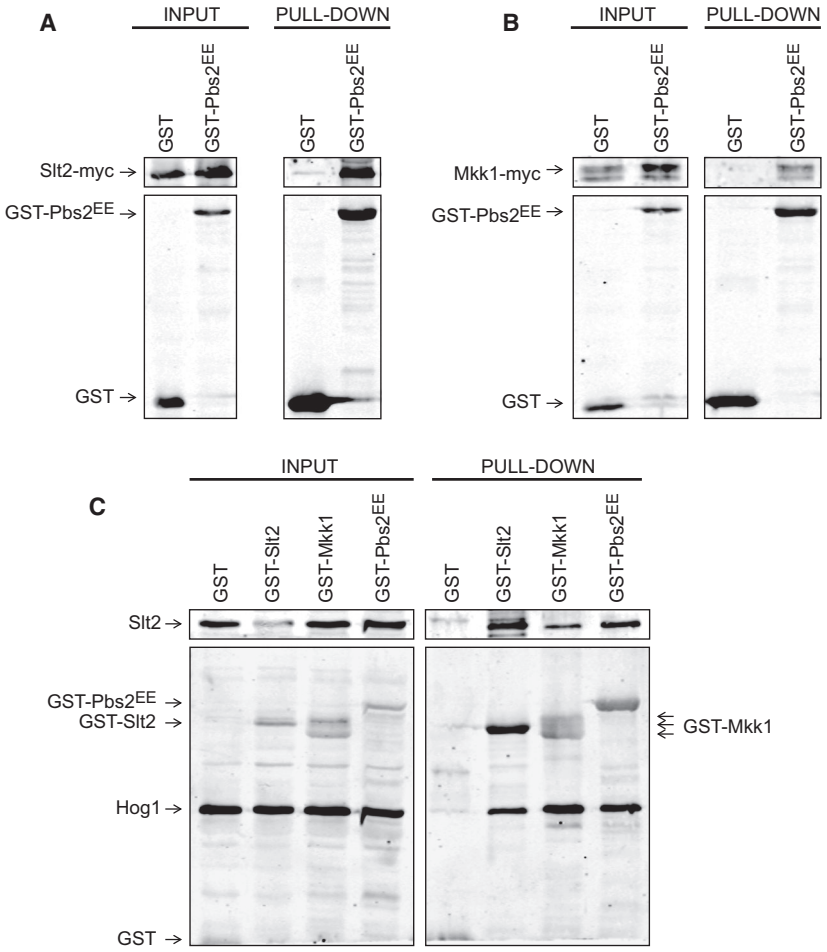

Fig. 8. The MAPKKs and MAPKs of the HOG and CWI pathways physically interact, forming a complex. The strains BY4741 *SLT2-6MYC* (A) and BY4741 *MKK1-6MYC* (B) were transformed with the plasmid pEG(KG)-*PBS2*^{EE} expressing GST-fused Pbs2^{EE}, or pEG(KG) expressing GST alone under control of the *GAL1* promoter; and the strain BY4741 (C) was transformed with plasmids expressing Slt2 (pEG(KG)-*SLT2*), Mkk1 (pEG(KG)-*MKK1*) or Pbs2^{EE} (pEG(KG)-*PBS2*^{EE}) fused to GST under control of the *GAL1* promoter. Transformants were grown in SG Ura– at 30 °C for 6 h, and cell extracts (input) were incubated with glutathione-Sepharose beads to purify GST complexes (pull-down). Slt2-myc (A), Mkk1-myc (B), endogenous Hog1 and Slt2 (C) and GST or the indicated GST-fused proteins (A–C) were detected with anti-myc, anti-Hog1 anti-Slt2 and anti-GST antibodies, respectively. Representative blots from two (A, B) and three (C) different experiments are shown.

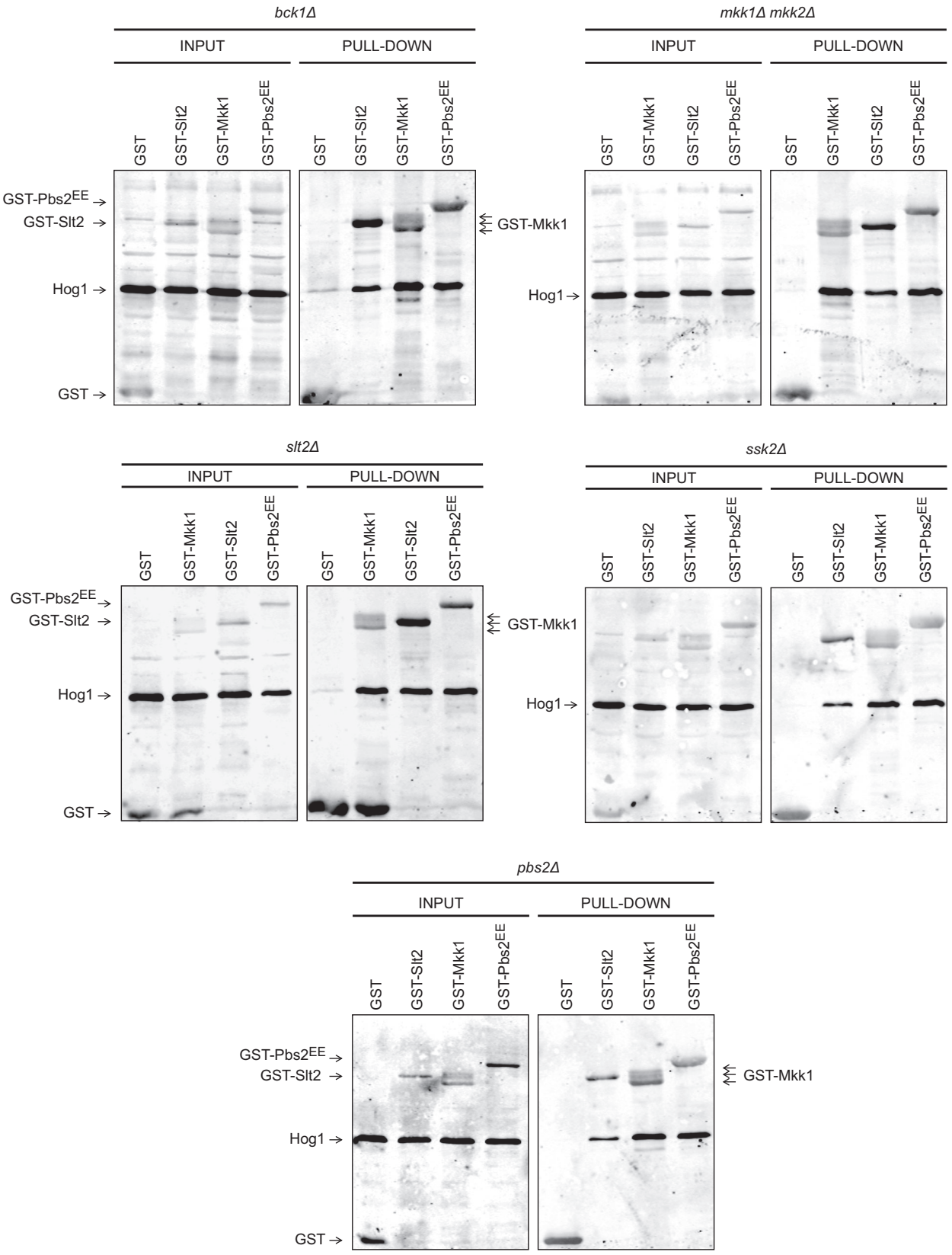

Fig. 9. Bck1, Mkk1/Mkk2, Slt2, Ssk2 and Pbs2 are not necessary for the physical interaction between components of the HOG and CWI pathways. BY4741 (WT) and the isogenic *bck1Δ*, *mkk1Δmkk2Δ*, *slt2Δ*, *ssk2Δ* and *pbs2Δ* mutant strains were transformed with plasmids expressing Mkk1 (pEG(KG)-*MKK1*), Slt2 (pEG(KG)-*SLT2*) or Pbs2^{EE} (pEG(KG)-*PBS2*^{EE}) fused to GST under control of the *GAL1* promoter. Transformants were grown in SG Ura– at 30 °C for 6 h, and cell extracts (input) were incubated with glutathione-Sepharose beads to purify GST complexes (pull-down). Hog1 and GST-fused proteins were detected with anti-Hog1 and anti-GST antibodies, respectively. Representative blots from two experiments are shown.

induced promoter would create a positive feedback circuit that, when triggered, would ultimately lead to growth inhibition. This was the case, as exposure of cells carrying the so-called IPAC to very low concentrations of a cell wall-altering agent, such as Congo red, inhibited yeast growth. This phenotype clearly relies on the integrity of the loop, since the lack of Rlm1 abolishes the IPAC-induced growth inhibition. The effect on growth was concomitant with high Slt2 phosphorylation levels and Mlp1 transcriptional induction, which indicates that the IPAC strongly increases the level of signalling and confers cell wall stress hypersensitivity. Results obtained from both readouts indicate that a sustained increase of threefold or fourfold over the wild-type CWI response is enough to confer lethality. We also found that a very transient stress, such as that provoked by hypotonic shock, sparked the positive feedback loop in a very fast manner, but also decayed rapidly in both wild-type and IPAC-containing cells, suggesting that this circuit does not promote bistability [33].

It is important to stress the potential power of the IPAC for drug discovery: on the one hand, as a highly sensitive testbed for finding novel antifungal molecules that alter the cell wall; on the other hand, to screen for MAPK signalling inhibitors based on their ability to prevent death in IPAC-containing cells subjected to CWI pathway stimulation. Besides potential applications as antiproliferative drugs in humans, such MAPK inhibitors could be used as synergistic antifungal drugs with known cell wall-targeted compounds, due to their ability to hinder the CWI pathway compensatory mechanism.

The IPAC is also a powerful tool for identifying subtle modulators of signalling, the deficiency of which does not promote a sensitivity phenotype and, therefore, is difficult to identify in phenotypic screenings. Exploiting the IPAC, we have found several genes, such as the two histone deacetylases Hos2 and Snt1 of the Set3 complex (Set3C) [34] that, when mutated, allowed IPAC-bearing cells to grow under cell surface stress. Set3C is important in regulating gene induction after changes in carbon sources [35], nitrogen starvation [34] and DNA damage [36]. Furthermore, this complex was found to signal secretory stress through the CWI pathway, as *HOS2* or *SNT1* deletion abrogated Slt2 phosphorylation in response to tunicamycin and provoked sensitivity to tunicamycin or 1,4-DTT [37]. Although *hos1* and *snt1* mutants do not show sensitivity to compounds such as SDS, zymolyase and Congo red, our results suggest the involvement of this complex in the response of the CWI pathway to plasma membrane and cell wall stress and suggest that the role of this complex within the CWI pathway merits further research.

The necessity of Pfk26 for full signalling through the CWI pathway is another interesting point to stress. Pfk26 is one of the two isoforms of 6-phosphofructo-2-kinase, responsible for the synthesis of fructose-2, 6-bisphosphate, a strong allosteric regulator of the glycolytic enzyme phosphofructokinase. Remarkably, the main target of phosphorylation among the enzymes regulating the yeast carbon metabolism is Pfk26, which can be considered as a phosphorylation hub [38]. In fact, Pkc1 phosphorylates Pfk26, causing its inactivation [39]. The consequent reduction of glycolysis has been proposed to lead to an accumulation of glucose-6-phosphate for the synthesis of glucan, as part of the cellular response to stress [38]. Moreover, nonallosteric phosphofructokinase mutants, that is insensitive to fructose-2,6-bisphosphate activation, were affected in sensitivity towards caffeine and Congo red [40]. Our results reinforce the idea that strong connections between the central carbon metabolism and cell wall regulation exist, as indicated by the CWI defects observed in mutants lacking the SNF1 complex [41].

Other mutants identified in the IPAC-based screening were the mitochondrial translocator Flx1, which catalyses the movement of the redox cofactor FAD across the mitochondrial membrane [42], and Tim18, an integral component of the translocase of the mitochondrial inner membrane complex TIM22 [43,44]. These results suggest the important role of mitochondrial function for signalling through this route. Interestingly, Srv2 also appeared as a protein important for full signalling through the pathway. Recently, Srv2 was shown to modulate yeast mitochondrial morphology and respiration by regulating actin assembly [45]. All this evidence suggests the relationship between mitochondrial activity and the CWI pathway and is

consistent with the reported regulation of mitochondrial fission by this pathway through cyclin C [46].

Among the signalling proteins identified using the IPAC tool, Ssk2 is of special interest. Although the *ssk2*Δ mutant is not SDS-sensitive, the hypersensitivity of this circuit for monitoring signalling has unveiled the role of Ssk2 as an input for the CWI MAPK in response to SDS. Some reports indicate that Hog1 may be activated by an alternative mechanism to the known sensors of the Sho1 and Sln1 branches, and that Ssk2 could be activated by an alternative route as an additional input for Hog1 phosphorylation under severe hyperosmotic stress [47,48]. However, phosphorylation of this MAPK in the absence of the known sensors of both branches fails to induce a protective response due to a diminished transcription activity of hyperosmolarity-responsive genes and defects in cell cycle regulation [49]. It is therefore tempting to speculate that one of the main roles of this alternative pathway could be to feed the CWI pathway.

Ssk2 binds actin and seems to sense disassembly of the actin cytoskeleton after osmotic stress [50]. Since the function of Ssk2 affects actin and MAPK signalling, Ssk2 makes an excellent candidate for coordinating these two cellular processes. The existence of proteins acting as actin sensors has been documented: for example, the mammalian transcription factors SRF and MRTF, which are maintained in an inactive conformation in the cytoplasm at high concentrations of G-actin [51]. If Ssk2 senses actin disorganisation, it would signal to Slt2 via Pbs2-Hog1 in response to other stimuli that promote actin cytoskeleton depolarisation, such as Congo red. This is indeed the case, as *ssk2*Δ or *hog1*Δ mutants show a reduced signalling through the CWI pathway in response to Congo red. However, the Congo red-induced signalling is able to trigger IPAC-induced lethality, even in *ssk2*Δ mutants, indicating that the putative sensing of actin by Ssk2 is not the only input for Slt2 activation in such conditions. In contrast, most of the signalling flows through the Ssk2-Hog1-Slt2 alternative pathway in the case of SDS. In agreement with this, the response to SDS is Rom2-independent, whereas Rom2-mediated CWI canonical pathway mostly conveys the signalling induced by Congo red.

Our results indicate that the Ssk2-mediated signalling unveiled herein acts in addition to its role in repairing the actin cytoskeleton. Amberg's group showed that Ssk2 works in the actin recovery pathway independently of the HOG pathway, but it requires Bni1, Pea2 or Bud6 [17]. However, the Ssk2-induced CWI activation pathway is mediated by the Pbs2-Hog1 module and does not require any of these proteins (data not shown). An attractive possibility is that Ssk2 is activated by actin depolarisation and participates in actin repolarisation, but also in signalling to Pbs2-Hog1, which ultimately will lead to CWI activation. Interestingly, actin binding stimulates the relocalisation of Ssk2 from the cytoplasm to the mother bud neck [50]. Furthermore, inactive Pbs2 localises at the mother bud neck during osmostress [52], and key components of the CWI pathway such as Pkc1, Slt2 and the sensors Wsc1 and Wsc2 also display a polarised localisation at the cytokinetic bud neck [53,54]. Therefore, it is tempting to speculate that Ssk2 relocalisation to the bud neck following SDS stress would allow activated Hog1 to impinge on the CWI pathway. This is supported by our finding of physical interactions among the components of the CWI and HOG MAPK modules. Formation of protein complexes composed of these components would also explain some of the crosstalks observed between these two pathways [12,13].

In summary, we demonstrate the feasibility of generating powerful tools for a better understanding of signalling pathways by expressing synthetic positive feedback loops that result in growth inhibition.

Materials and methods

Yeast strains and culture conditions

Unless otherwise stated, the yeast strains used in this work were *S. cerevisiae* BY4741 (*MAT*a *his3*Δ*1 leu2*Δ*0 met15*Δ*0 ura3*Δ0) and the isogenic *kanMX4* deletion mutants. These mutants, including those used for the screening (Table S1), were from Euroscarf. Wild-type BY4742 (*MAT*a *his3*Δ*1 leu2*Δ*0 met15*Δ*0 ura3*Δ0) and its isogenic *nmd5*Δ::*HIS3* mutant strain APY276 [55], PW245 strain (*HOG1-GFP-TRP1*) and the isogenic PW349 (*HOG1-GFP-TRP1 nmd5::URA3*) [56], YMF3 (BY4741 *SLT2-6MYC*) [57] and YMJ21 (BY4741 *MKK1-6MYC*) [58] have been previously described.

Yeast cultures were performed in yeast extract–bacto-peptone–dextrose (YPD, 1% yeast extract, 2% peptone, 2% dextrose), selective synthetic dextrose media (SD, 0.17% yeast nitrogen base, 0.5% ammonium sulfate, 2% dextrose, supplemented with the required amino acids), selective synthetic galactose media (SG, the same as SD but with galactose instead of dextrose) or selective synthetic raffinose media (SR, the same as SD but with raffinose instead of dextrose), either broth or agar.

DNA manipulation and plasmids

General DNA methods were performed using standard techniques.

To obtain plasmid YCplac111-IPAC, the restriction sites *Psp*OM1 and *Bam*H1 were first introduced by PCR into the *LEU2*-based centromeric plasmid YCplac111 [59] by cloning the *Eco*R1-*Hind*III DNA fragment amplified by PCR with primers *Eco*R1-*Psp*OM1 (5′-GGGAATTCGGGCCCATGCCGTTTACATTTCAGATC-3′) and *Bam*H1-*Hind*III (5′-CGGATCCCTAAAGCTTCCCGTTATTATTATAATTAAACATC-3′) using the plasmid pGEX-KG-SteC as template [60]. Then, the IPAC cassette, previously constructed by successive cloning of the *MLP1* promoter, PCR-amplified from genomic DNA with oligonucleotides 5′-CCCCG*GGGCC*AC AACAAGAACGTGGGCGATAC-3′ (*PspOM*I) and 5′-CCC C*CTCGAG*CATTTAATTGTGAATCTTTCTTCG-3′ (*Xho*I), the *MKK1*^{S386P} coding sequence, PCR-amplified with oligonucleotides 5′-CCCGTCGA*CTCGAG*ATGGCTTCACTGTTCA GACC-3′ (*Xho*I) and 5′-CCC*GTCGAC*TTAATCTTTCCA GCACTTCC-3′ (*Sal*I) using plasmid as pNV7-MKK1^{P386} [25] as template, and the *ADH1* terminator, PCR-amplified with oligonucleotides 5′-CCCCGGATCC*GTCGAC*CCTGAGTA ATAAGCG-3′ (*Sal*I) and 5′-CCCCCGGATCCCGGTGG TGGTCAATAAG-3′ (*Bam*H1) from genomic DNA, was subcloned into *Psp*OMI and *Bam*H1 sites of YCplac111. pHR70-IPAC was obtained by cloning the *Eco*R1-*Bam*H1 containing the genetic circuit from YCplac111-IPAC into the *URA3*-based centromeric plasmid PHR70 [19].

pEG(KG)-PBS2^{EE} was constructed by overlapping PCR amplifying the *PBS2* gene with oligonucleotides 5′-CCCGT CGACTCGAGATGGAAGACAAGTTTGC-3′ (*SalI*) and 5′-CCC GTCGACCTATAAACCACCCATATG-3′ (*SalI*) and the mutagenic primers 5′-CTGGTAATTTGGTGGCAG AATTAGCGAAGGAAAATATTGGTTGTCAGTC-3′ and 5′-GACTGACAACCAATATTTTCCTTCGCTAATTCTGC CACCAAATTACCAG-3′. These primers led to the replacement of amino acids Ser514 and Thr518 of Pbs2 by Glu [31]. Thus, this PBS2^{EE} allele contained substitution mutations that were similar to the changes to Asp previously described that mimic the activating phosphorylation events and activate Pbs2p without the involvement of upstream elements (Ssk2p, Ssk22p and Sho1p) [31].

Plasmids pRS416-*HOG1-GFP*, pRS416-*HOG1*^{TAYA}*-GFP* and pRS416-*HOG1*^{KM}*-GFP* [10], pEG(KG), pEG(KG)-SLT2, pEG(KG)-*MKK1* [61], p*MLP1-lacZ* [62], pCW194 and pRS413-p*GAL1-ssk2*ΔN [32] and pVD67 [30] have been described previously.

Halo sensitivity assay

Yeast cells were cultured overnight at 30 °C in SD Leu– pH 6.5 liquid medium. A volume of 100 μL of this saturated culture was resuspended in 4 mL of SD Leu– pH 6.5 with 0.7% agar and poured onto SD Leu– pH 6.5 plates. Sterile 6-mm-diameter paper discs were impregnated with 20 μL of the indicated solution and placed over the top-layer agar. Plates were incubated at 30 °C for 48 h, and the generated inhibition halos were photographed.

Multiwell plate sensitivity assay

Yeast cells from an overnight culture were diluted to a final optical density $(OD)_{595}$ of 0.01 and cultured at 30 °C in multiwell plates containing YPD with serial dilutions of zymolyase at the indicated concentrations. Growth was determined as OD_{595} after 12.5 h of incubation using a Bio-Rad 680 microplate reader (Bio-Rad, Hercules, CA, USA).

Hyperosmotic shock

Yeast cells were cultured overnight at 30 °C in YPD and then transferred to the same fresh medium for a final OD_{595} of 0.3, cultured for an additional 2 h, collected by centrifugation and then resuspended in YPD containing 1 M sorbitol.

Hypotonic shock

Yeast cells were cultured overnight at 24 °C in YPD containing 1 M sorbitol and then transferred to the same fresh medium for a final OD_{595} of 0.3, cultured for an additional 3 h, collected by centrifugation and then resuspended in YPD.

Yeast drop dilution growth assays

Growth assays on solid media were performed by culturing cells in YPD or selective SD medium to an OD_{595} of 0.5 and spotting samples (5 μL) of 10-fold dilutions of the cell suspensions onto the surface of plates followed by incubation at 30 °C for 48–72 h.

Genetic screening on a subcollection of mutant strains of *S. cerevisiae*

A subcollection of mutants (Table S1) was distributed in 96-well plates and transformed with the plasmid YCplac111-IPAC. The plates were incubated at 30 °C for 72 h until the appearance of sediment in the well, corresponding to transformed yeasts. Five microlitres of these cultures was diluted into new multiwell plates containing 200 μL of SD medium lacking leucine to inoculate plates of solid SD medium lacking leucine and containing Congo red (10 $\mu g \cdot mL^{-1}$), zymolyase 100 T (150 $\mu g \cdot mL^{-1}$) or SDS (0.01%) with a pin replicator. Plates were incubated for 48 h at 30 °C. After incubation, those mutants capable of suppressing the growth inhibition phenotype caused by the IPAC were obtained again from the collection stock and transformed with the plasmid pHR70-IPAC. Their ability to grow on SD plates without uracil in the absence or presence of the same compounds and concentrations at 30 °C for 48 h was confirmed by drop growth assays.

Preparation of yeast extracts and immunoblotting analysis

The procedures used for obtaining yeast extracts, fractionation by SDS/PAGE and transfer to nitrocellulose membranes have been described previously [19]. Mouse monoclonal anti-Slt2 (Santa Cruz Biotechnology; Dallas, TX, USA), rabbit polyclonal anti-Hog1 (Santa Cruz Biotechnology), rabbit monoclonal anti-phospho-p44/42 (Thr202/Tyr204) antibody (Cell Signaling, Danvers, MA, USA), rabbit monoclonal anti-phospho-p38 (Cell Signaling), mouse monoclonal anti-GFP (Clontech, Kyoto; Japan), mouse monoclonal anti-myc (Millipore, Burlington, MA, USA), rabbit polyclonal anti-GST (Santa Cruz Biotechnology) and rabbit polyclonal anti-G6PDH (Sigma, St. Louis, MO, USA) were used to recognise Slt2, Hog1, dually phosphorylated Slt2, dually phosphorylated Hog1, GFP, myc, GST and G6PDH as a loading control, respectively. The primary antibodies were detected using a fluorescently conjugated secondary antibody with an Odyssey Infrared Imaging System (LI-COR Biosciences, Lincoln, NE, USA).

Copurification experiments

Yeast cells expressing *GAL1*-driven GST-fused proteins (Slt2, Mkk1, $Pbs2^{EE}$ and Hog1) were cultured overnight at 30 °C in selective synthetic SR medium lacking uracil, refreshed in selective synthetic SG medium lacking uracil at OD_{595} = 0.3 and cultured at 30 °C for an additional 6 h. Cells were collected on ice, pelleted and resuspended in cold lysis buffer [50 mM Tris/HCl (pH 7.5), 5 mM EDTA (pH 8), 150 mM NaCl, 50 mM NaF, 5 mM sodium pyrophosphate, 10% glycerol, 0.1% NP-40, 50 mM β-glycerol phosphate, 1 mM sodium orthovanadate] supplemented with 1 mM phenylmethylsulfonyl fluoride (PMSF) and protease inhibitor mixture (Thermo Scientific, Waltham, MA, USA). Cells were glass-bead-lysed and whole extracts clarified and incubated with glutathione-Sepharose beads (GE Healthcare, Chicago, IL, USA) overnight at 4 °C. Beads were extensively washed with lysis buffer lacking PMSF and protease inhibitor mixture. 2× SDS loading buffer was added; proteins were boiled for 5 min and analysed by SDS/PAGE and immunoblotting.

β-Galactosidase activity assays

β-Galactosidase activity was determined as described previously [62]. In brief, extracts were obtained by breaking cells with glass beads. β-Galactosidase activity was spectrophotometrically determined at 415 nm by using *o*-nitrophenyl-β-D-galactopyranoside as substrate and expressed as nmoles of *o*-nitrophenol·min^{-1}·mg^{-1} of total protein, as quantified by Bradford assay.

Microscopy techniques

For GFP *in vivo* fluorescence microscopy, cells were cultured in SD or YPD overnight at 24 °C. They were refreshed to an OD_{595} = 0.3 with YPD and incubated for 1.5 h in a shaker at 24 °C. Then, 0.9 M NaCl or SDS 0.01% was added to the cultures and samples were taken at different time points and analysed by fluorescence microscopy.

Cells were visualised in an Eclipse TE2000U microscope (Nikon, Tokyo, Japan) using the appropriate sets of filters. Digital images were acquired with Orca C4742-95-12ER charge-coupled device camera (Hamamatsu, Shizuoka, Japan) and processed with the HCIMAGE software (Hamamatsu).

Acknowledgements

We thank Sergio Peisajovich, Wendel Lim, Henrick Dohlman, David Levin and Javier Arroyo for materials used in this study. We also thank colleagues from Unit 3 of the Departamento de Microbiología y Parasitología at UCM for useful comments and discussion throughout the work. We acknowledge the Servicio de Genómica y Proteómica (UCM, Madrid, Spain) for DNA sequencing. This work was supported by grant BIO2016-75030-P from Ministerio de Economía y Competitividad (Spain), and S2017/BMD-3691 (InGEMICS-CM) funded by Comunidad de Madrid (Spain) and European Structural and Investment Funds. EA-R was recipient of a FPI contract from Ministerio de Ciencia e Innovación (Spain). EJ-G is recipient of a predoctoral contract from Universidad Complutense de Madrid. EA-C is recipient of a laboratory assistant contract from Comunidad Autónoma de Madrid and cofunded by Fondo Social Europeo within Programa Operativo de Empleo Juvenil and Iniciativa de Empleo Juvenil (YEI).

Conflicts of interest

The authors declare no conflict of interest.

Author contributions

EJ-G, EA-R, EA-C and TF-A conducted the experiments and analysed the results. MM analysed the results and wrote the paper. HM conceived the idea for the project, analysed the results and wrote the paper with MM.

References

1 Krishna M & Narang H (2008) The complexity of mitogen-activated protein kinases (MAPKs) made simple. *Cell Mol Life Sci* **65**, 3525–3544.

2 Chen RE & Thorner J (2007) Function and regulation in MAPK signaling pathways: Lessons learned from the yeast *Saccharomyces cerevisiae*. *Biochim Biophys Acta* **1773**, 1311–1340.
3 Levin DE (2011) Regulation of cell wall biogenesis in *Saccharomyces cerevisiae*: the cell wall integrity signaling pathway. *Genetics* **189**, 1145–1175.
4 Jung US, Sobering AK, Romeo MJ & Levin DE (2002) Regulation of the yeast Rlm1 transcription factor by the Mpk1 cell wall integrity MAP kinase. *Mol Microbiol* **46**, 781–789.
5 Garcia R, Bermejo C, Grau C, Perez R, Manuel Rodriguez-Pena J, Francois J, Nombela C & Arroyo J (2004) The global transcriptional response to transient cell wall damage in *Saccharomyces cerevisiae* and its regulation by the cell integrity signaling pathway. *J Biol Chem* **279**, 15183–15195.
6 Jimenez-Gutierrez E, Alegria-Carrasco E, Sellers-Moya A, Molina M & Martin H (2019) Not just the wall: the other ways to turn the yeast CWI pathway on. *Int Microbiol* **23**, 107–119.
7 Saito H & Posas F (2012) Response to hyperosmotic stress. *Genetics* **192**, 289–318.
8 Brewster JL &Gustin MC (2014) Hog 1: 20 years of discovery and impact. *Sci Signal* **7**, re7.
9 Hohmann S (2015) An integrated view on a eukaryotic osmoregulation system. *Curr Genet* **61**, 373–382.
10 Ferrigno P, Posas F, Koepp D, Saito H & Silver PA (1998) Regulated nucleo/cytoplasmic exchange of HOG1 MAPK requires the importin beta homologs NMD5 and XPO1. *EMBO J* **17**, 5606–5614.
11 de Nadal E & Posas F (2015) Osmostress-induced gene expression–a model to understand how stress-activated protein kinases (SAPKs) regulate transcription. *FEBS J* **282**, 3275–3285.
12 Garcia-Rodriguez LJ, Valle R, Duran A & Roncero C (2005) Cell integrity signaling activation in response to hyperosmotic shock in yeast. *FEBS Lett* **579**, 6186–6190.
13 Bermejo C, Rodriguez E, Garcia R, Rodriguez-Pena JM, Rodriguez de la Concepcion ML, Rivas C, Arias P, Nombela C, Posas F & Arroyo J (2008) The sequential activation of the yeast HOG and SLT2 pathways is required for cell survival to cell wall stress. *Mol Biol Cell* **19**, 1113–1124.
14 Leng G & Song K (2016) Direct interaction of Ste11 and Mkk1/2 through Nst1 integrates high-osmolarity glycerol and pheromone pathways to the cell wall integrity MAPK pathway. *FEBS Lett* **590**, 148–160.
15 Delley PA & Hall MN (1999) Cell wall stress depolarizes cell growth via hyperactivation of RHO1. *J Cell Biol* **147**, 163–174.
16 Kono K, Saeki Y, Yoshida S, Tanaka K & Pellman D (2012) Proteasomal degradation resolves competition between cell polarization and cellular wound healing. *Cell* **150**, 151–164.
17 Bettinger BT, Clark MG & Amberg DC (2007) Requirement for the polarisome and formin function in Ssk2p-mediated actin recovery from osmotic stress in *Saccharomyces cerevisiae*. *Genetics* **175**, 1637–1648.
18 Gerits N, Kostenko S & Moens U (2007) *In vivo* functions of mitogen-activated protein kinases: conclusions from knock-in and knock-out mice. *Transgenic Res* **16**, 281–314.
19 Martin H, Rodriguez-Pachon JM, Ruiz C, Nombela C & Molina M (2000) Regulatory mechanisms for modulation of signaling through the cell integrity Slt2-mediated pathway in *Saccharomyces cerevisiae*. *J Biol Chem* **275**, 1511–1519.
20 Lake D, Correa SA & Muller J (2016) Negative feedback regulation of the ERK1/2 MAPK pathway. *Cell Mol Life Sci* **73**, 4397–4413.
21 Brandman O & Meyer T (2008) Feedback loops shape cellular signals in space and time. *Science* **322**, 390–395.
22 Blount BA, Weenink T & Ellis T (2012) Construction of synthetic regulatory networks in yeast. *FEBS Lett* **586**, 2112–2121.
23 Furukawa K & Hohmann S (2013) Synthetic biology: lessons from engineering yeast MAPK signalling pathways. *Mol Microbiol* **88**, 5–19.
24 Ingolia NT & Murray AW (2007) Positive-feedback loops as a flexible biological module. *Curr Biol* **17**, 668–677.
25 Watanabe Y, Irie K & Matsumoto K (1995) Yeast RLM1 encodes a serum response factor-like protein that may function downstream of the Mpk1 (Slt2) mitogen-activated protein kinase pathway. *Mol Cell Biol* **15**, 5740–5749.
26 Davenport KR, Sohaskey M, Kamada Y, Levin DE & Gustin MC (1995) A second osmosensing signal transduction pathway in yeast Hypotonic shock activates the PKC1 protein kinase-regulated cell integrity pathway. *J Biol Chem* **270**, 30157–30161.
27 Bermejo C, Garcia R, Straede A, Rodriguez-Pena JM, Nombela C, Heinisch JJ & Arroyo J (2010) Characterization of sensor-specific stress response by transcriptional profiling of wsc1 and mid2 deletion strains and chimeric sensors in *Saccharomyces cerevisiae*. *OMICS* **14**, 679–688.
28 Kuranda K, Leberre V, Sokol S, Palamarczyk G & Francois J (2006) Investigating the caffeine effects in the yeast *Saccharomyces cerevisiae* brings new insights into the connection between TOR, PKC and Ras/cAMP signalling pathways. *Mol Microbiol* **61**, 1147–1166.
29 Andrews PD & Stark MJ (2000) Dynamic, Rho1p-dependent localization of Pkc1p to sites of polarized growth. *J Cell Sci* **113**, 2685–2693.

30 Denis V & Cyert MS (2005) Molecular analysis reveals localization of *Saccharomyces cerevisiae* protein kinase C to sites of polarized growth and Pkc1p targeting to the nucleus and mitotic spindle. *Eukaryot Cell* **4**, 36–45.
31 Wurgler-Murphy SM, Maeda T, Witten EA & Saito H (1997) Regulation of the *Saccharomyces cerevisiae* HOG1 mitogen-activated protein kinase by the PTP2 and PTP3 protein tyrosine phosphatases. *Mol Cell Biol* **17**, 1289–1297.
32 Nagiec MJ & Dohlman HG (2012) Checkpoints in a yeast differentiation pathway coordinate signaling during hyperosmotic stress. *PLoS Genet* **8**, e1002437.
33 Pomerening JR (2008) Uncovering mechanisms of bistability in biological systems. *Curr Opin Biotechnol* **19**, 381–388.
34 Pijnappel WW, Schaft D, Roguev A, Shevchenko A, Tekotte H, Wilm M, Rigaut G, Seraphin B, Aasland R & Stewart AF (2001) The *S cerevisiae* SET3 complex includes two histone deacetylases, Hos2 and Hst1, and is a meiotic-specific repressor of the sporulation gene program. *Genes Dev* **15**, 2991–3004.
35 Kim T, Xu Z, Clauder-Munster S, Steinmetz LM & Buratowski S (2012) Set3 HDAC mediates effects of overlapping noncoding transcription on gene induction kinetics. *Cell* **150**, 1158–1169.
36 Kim T & Buratowski S (2009) Dimethylation of H3K4 by Set1 recruits the Set3 histone deacetylase complex to 5' transcribed regions. *Cell* **137**, 259–272.
37 Cohen TJ, Mallory MJ, Strich R & Yao TP (2008) Hos2p/Set3p deacetylase complex signals secretory stress through the Mpk1p cell integrity pathway. *Eukaryot Cell* **7**, 1191–1199.
38 Tripodi F, Nicastro R, Reghellin V & Coccetti P (2015) Post-translational modifications on yeast carbon metabolism: Regulatory mechanisms beyond transcriptional control. *Biochim Biophys Acta* **1850**, 620–627.
39 Dihazi H, Kessler R & Eschrich K (2001) Phosphorylation and inactivation of yeast 6-phosphofructo-2-kinase contribute to the regulation of glycolysis under hypotonic stress. *Biochemistry* **40**, 14669–14678.
40 Rodicio R, Strauss A & Heinisch JJ (2000) Single point mutations in either gene encoding the subunits of the heterooctameric yeast phosphofructokinase abolish allosteric inhibition by ATP. *J Biol Chem* **275**, 40952–40960.
41 Backhaus K, Rippert D, Heilmann CJ, Sorgo AG, de Koster CG, Klis FM, Rodicio R & Heinisch JJ (2013) Mutations in SNF1 complex genes affect yeast cell wall strength. *Eur J Cell Biol* **92**, 383–395.
42 Tzagoloff A, Jang J, Glerum DM & Wu M (1996) FLX1 codes for a carrier protein involved in maintaining a proper balance of flavin nucleotides in yeast mitochondria. *J Biol Chem* **271**, 7392–7397.
43 Kerscher O, Sepuri NB & Jensen RE (2000) Tim18p is a new component of the Tim54p-Tim22p translocon in the mitochondrial inner membrane. *Mol Biol Cell* **11**, 103–116.
44 Koehler CM, Murphy MP, Bally NA, Leuenberger D, Oppliger W, Dolfini L, Junne T, Schatz G & Or E (2000) Tim18p, a new subunit of the TIM22 complex that mediates insertion of imported proteins into the yeast mitochondrial inner membrane. *Mol Cell Biol* **20**, 1187–1193.
45 Chen YC, Cheng TH, Lin WL, Chen CL, Yang WY, Blackstone C & Chang CR (2019) Srv2 is a pro-fission factor that modulates yeast mitochondrial morphology and respiration by regulating actin assembly. *iScience* **11**, 305–317.
46 Jin C, Strich R & Cooper KF (2014) Slt2p phosphorylation induces cyclin C nuclear-to-cytoplasmic translocation in response to oxidative stress. *Mol Biol Cell* **25**, 1396–1407.
47 Van Wuytswinkel O, Reiser V, Siderius M, Kelders MC, Ammerer G, Ruis H & Mager WH (2000) Response of *Saccharomyces cerevisiae* to severe osmotic stress: evidence for a novel activation mechanism of the HOG MAP kinase pathway. *Mol Microbiol* **37**, 382–397.
48 Zhi H, Tang L, Xia Y & Zhang J (2013) Ssk1p-independent activation of Ssk2p plays an important role in the osmotic stress response in *Saccharomyces cerevisiae*: alternative activation of Ssk2p in osmotic stress. *PLoS ONE* **8**, e54867.
49 Vazquez-Ibarra A, Subirana L, Ongay-Larios L, Kawasaki L, Rojas-Ortega E, Rodriguez-Gonzalez M, de Nadal E, Posas F & Coria R (2018) Activation of the Hog1 MAPK by the Ssk2/Ssk22 MAP3Ks, in the absence of the osmosensors, is not sufficient to trigger osmostress adaptation in *Saccharomyces cerevisiae*. *FEBS J* **285**, 1079–1096.
50 Yuzyuk T, Foehr M & Amberg DC (2002) The MEK kinase Ssk2p promotes actin cytoskeleton recovery after osmotic stress. *Mol Biol Cell* **13**, 2869–2880.
51 Fernandez-Barrera J & Alonso MA (2018) Coordination of microtubule acetylation and the actin cytoskeleton by formins. *Cell Mol Life Sci* **75**, 3181–3191.
52 Reiser V, Salah SM & Ammerer G (2000) Polarized localization of yeast Pbs2 depends on osmostress, the membrane protein Sho1 and Cdc42. *Nat Cell Biol* **2**, 620–627.
53 van Drogen F & Peter M (2002) Spa2p functions as a scaffold-like protein to recruit the Mpk1p MAP kinase module to sites of polarized growth. *Curr Biol* **12**, 1698–1703.
54 Wilk S, Wittland J, Thywissen A, Schmitz HP & Heinisch JJ (2010) A block of endocytosis of the yeast cell wall integrity sensors Wsc1 and Wsc2 results in reduced fitness *in vivo*. *Mol Genet Genomics* **284**, 217–229.

55 Perez AM & Thorner J (2019) Septin-associated proteins Aim44 and Nis1 traffic between the bud neck and the nucleus in the yeast *Saccharomyces cerevisiae*. *Cytoskeleton (Hoboken)* **76**, 15–32.
56 Westfall PJ & Thorner J (2006) Analysis of mitogen-activated protein kinase signaling specificity in response to hyperosmotic stress: use of an analog-sensitive HOG1 allele. *Eukaryot Cell* **5**, 1215–1228.
57 Flandez M, Cosano IC, Nombela C, Martin H & Molina M (2004) Reciprocal regulation between Slt2 MAPK and isoforms of Msg5 dual-specificity protein phosphatase modulates the yeast cell integrity pathway. *J Biol Chem* **279**, 11027–11034.
58 Jimenez-Sanchez M, Cid VJ & Molina M (2007) Retrophosphorylation of Mkk1 and Mkk2 MAPKKs by the Slt2 MAPK in the yeast cell integrity pathway. *J Biol Chem* **282**, 31174–31185.
59 Gietz RD & Sugino A (1988) New yeast-*Escherichia coli* shuttle vectors constructed with *in vitro* mutagenized yeast genes lacking six-base pair restriction sites. *Gene* **74**, 527–534.
60 Fernandez-Pinar P, Aleman A, Sondek J, Dohlman HG, Molina M & Martin H (2012) The Salmonella Typhimurium effector SteC inhibits Cdc42-mediated signaling through binding to the exchange factor Cdc24 in *Saccharomyces cerevisiae*. *Mol Biol Cell* **23**, 4430–4443.
61 Soler M, Plovins A, Martin H, Molina M & Nombela C (1995) Characterization of domains in the yeast MAP kinase Slt2 (Mpk1) required for functional activity and in vivo interaction with protein kinases Mkk1 and Mkk2. *Mol Microbiol* **17**, 833–842.
62 Garcia R, Rodriguez-Pena JM, Bermejo C, Nombela C & Arroyo J (2009) The high osmotic response and cell wall integrity pathways cooperate to regulate transcriptional responses to zymolyase-induced cell wall stress in *Saccharomyces cerevisiae*. *J Biol Chem* **284**, 10901–10911.

Supporting information

Additional supporting information may be found online in the Supporting Information section at the end of the article.

Table S1. Yeast mutant strains included in the screened subcollection.